arXiv:2208.06542v1 [cond-mat.mtrl-sci] 13 Aug 2022

Ferroelectricity induced by the absorption of water molecules on double helix SnIP

Dan Liu[1]*, Ran Wei[1], Lin Han[1], Chen Zhu[1] and Shuai Dong[1]

[1]School of Physics, Southeast University, Nanjing 211189, China

August 16, 2022

Abstract

We study the ferroelectricity in a one-dimensional system composed of a double helix SnIP with absorbing water molecules. Our *ab initio* calculations reveal two factors that are critical to the electrical polarization. The first one is the orientation of polarized water molecules staying in the R2 region of SnIP. The second one is the displacement of I atom which roots from subtle interaction with absorbed water molecules. A reasonable scenario of polarization flipping is proposed in this study. In the scenario, the water molecule is rolling-up with keeping the magnitude of its electrical dipole and changing its direction, meanwhile, the displacement of I atoms is also reversed. Highly tunable polarization can be achieved by applying strain, with 26.5% of polarization enhancement by applying tensile strain, with only 4% degradation is observed with 4% compressive strain. Finally, the direct band gap is also found to be correlated with strain.

Keywords: ferroelectricity, 1D double helix, electrical polarization, DFT

PACS: 77.80.-e, 77.84.-s, 73.22.-f

1. Introduction

Since the first experimental discovery of ferroelectricity in Rochelle salt [1], in the past hundred years, for the perspective of application in sensors, actuators and memories, a wide range of ferroelectric (FE) materials have been intensively studied, such as the well known three dimensional (3D) $BaTiO_3$ [2]. Interest in new, low-dimensional ferroelectrics has also been growing rapidly due to their potential applications in electronics, such as recently emerged ferroelectric two-dimensional (2D) layered structures including group-VI monochalcogenides, In_2Se_3, $CuInP_2S_6$, etc [3–16]. Besides these intrinsic 2D FE materials, ferroelectricity can be also induced in non-FE 2D system through doping, manipulating defects and also fabricating heterojunctions. For example, the hydroxyl-decorated graphene systems exhibit a robust ferroelectricity [17–19]. The increasing demand in high density in electronic device requests the further miniaturization of FE materials. One method is to cut a one-dimensional (1D) nanoribbon from the traditional 3D or 2D FE materials. However, there are two obvious drawbacks of these 1D nanoribbons. One is the size of such nanoribbon is quite large. For example, graphene nanoribbons fabricated by etching graphene using high-resolution electron beam lithography range from 10 nm

*Corresponding author. E-mail: liudan2@seu.edu.cn

to 100 nm [20]. This size is much larger than typical 1D structures, such as the (10, 10) carbon nanotube (CNT) of which the diameter is only about 1.3 nm [21]. So these nanoribbons can not be categorized as real 1D ferroelectricity, and thus the reduction effect in electronic device size using these FE nanoribbons is limited. The second concern is about the stability of these nanoribbons, while cutting from their 3D or 2D parent compounds. The atoms staying on the edge are electrical unsaturated, which will result in a structural distortion and accordingly the FE behavior of these nanoribbons. In general, the optimum method to reduce the size and increase the density of electronic devices should be seeking real 1D ferroelectricity in atomic scale. Despite abundant 1D structures that have been explored since the successful synthesis of CNT [22], intrinsic 1D FE materials are rarely found [23–25]. In analogy with decorating graphene using hydroxyl to introduce electrical polarization, a similar effect may be expecting in existed 1D structures through doping of polarized molecules.

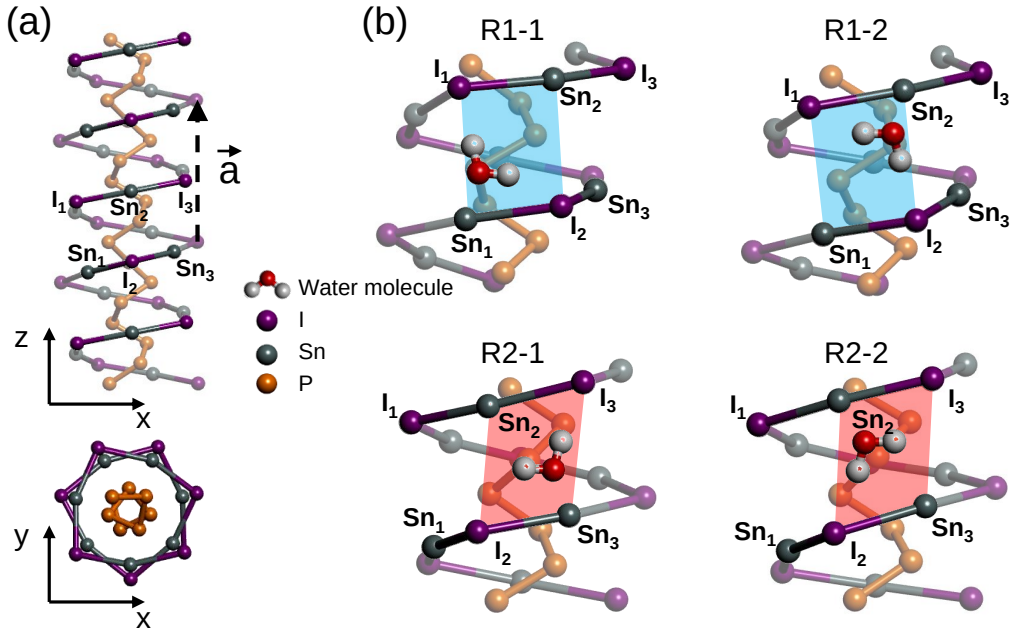


Fig. 1. Atomic structure of (a) 1D double-helix SnIP, (b) four configurations of one water molecule attaching on region R1 of SnIP highlighted by transparent blue area, on region R2 highlighted by red transparent red area. Black dashed arrow represents the vector of unit cell.

Water molecule is a very common polarized molecule around us. However, little attention has been focused on the ferroelectricity of water to date, because it is not easy to make water molecules form a well-organized arrangement. To solve the problem, we need to find an appropriate way to enforce water molecules to form an expected arrangement. Previous study reported a unique structure of quasi-1D water molecules confined in a 3D supramolecular architecture. When the water molecules are frozen into special forms, this quasi-1D water wire becomes ferroelectric [26]. In this study, we investigate the electric polarization in 1D double-helix SnIP [28,36] with absorption of water molecules. Our density functional theory (DFT) calculations reveal that there are two regions R1 and R2 in SnIP to anchor water molecules. And for each region, there are also two energetic degenerate configurations holding promise of the reversal of water molecule. We find that there are two factors contributing to the emergence of ferroelectricity in the system. One is the orientation of the polarized water molecules, the other is the displacement of ions in SnIP originating from the interaction between water molecules and SnIP. While flipping the orientation of water molecules from one degenerate configuration to the other, the displacement of ions of SnIP will also be reversed, which leads to the reversal of an entire electrical

dipole. The magnitude of polarization can be tuned mainly through applying tensile strain along the axis of SnIP, while almost remaining constant under compressive strain. The band gap of the system, remaining to be direct, can be tuned by the axial strain as well.

2. Theoretical method

Our calculations of the stability, equilibrium structure, polarization and energy changes during structural transformations have been performed using the density functional theory (DFT) as implemented in SIESTA code [29]. The 1D systems have been represented using periodic boundary conditions and separated by 20Å. We have used the nonlocal Perdew-Burke-Ernzerhof (PBE) [30] and Local-Density-Approximation (LDA) [42] exchange-correlation functional, norm-conserving Troullie-Martins pseudopotentials [31], and a local numerical double-ζ basis including polarization orbitals. The Brillouin zone of periodic structures has been sampled by a fine grid of 1×1×12 k-points for 1D structures [32]. We find the basis, k-point grid, and mesh cutoff energy of 180 Ry used in the Fourier representation of the self-consistent charge density to be fully converged, providing us with a precision in total energy of 2 meV/atom. Geometries have been optimized using the conjugate gradient (CG) method [33], until none of the residual Hellmann-Feynman forces exceeded 10^{-2} eV/Å. For the phonon spectrum calculation, we use a much smaller force tolerance of 10^{-3} eV/Å to get the optimized structure. The polarization is calculated using Berry phase method [34,35].

3. Results and Discussion

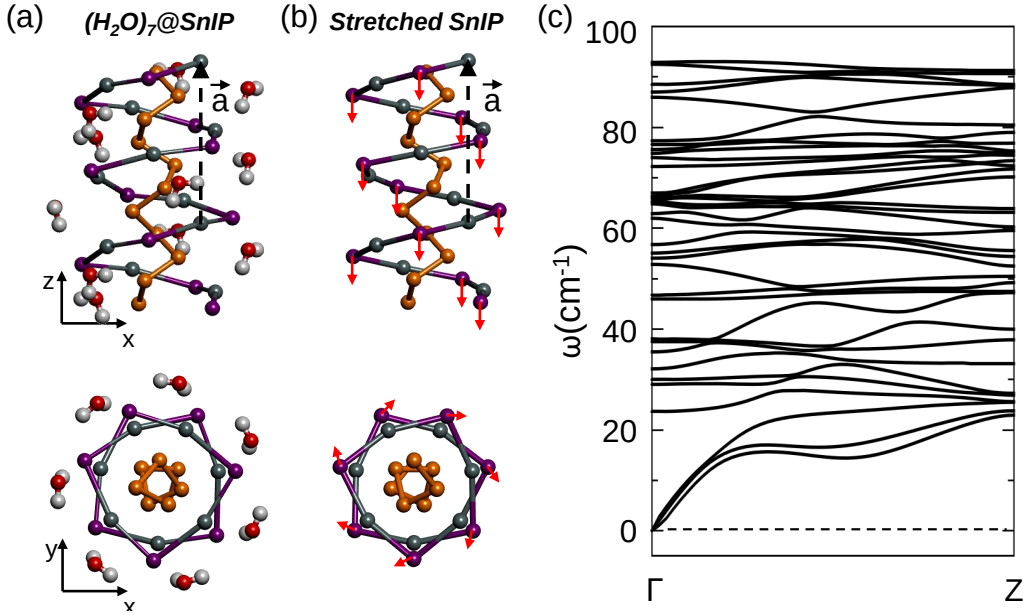


Fig. 2. Atomic structure of (a) $(H_2O)_7$@SnIP with 7 H_2O attaching on SnIP, (b) stretched SnIP with the same unit cell size of $(H_2O)_7$@SnIP in (a). (c) Phonon spectrum of $(H_2O)_7$@SnIP. The red arrow with solid line represent the shift of the atoms transforming the stretched SnIP in (b) to SnIP in $(H_2O)_7$@SnIP of (a).

Atomic structure of 1D double-helix SnIP and water@SnIP

The bunch of SnIP has been synthesized successfully in experiment [36]. The single rod of double-helix SnIP is composed of the inner Phosphorus (P) helix and the outer Tin(Sn)-Iodine(I) helix, which contains seven

P, Sn and I atoms in one primitive unit cell. The double helix of SnIP can be either right-handed or left-handed with the same energetic stability. Here, we focus on the right-handed SnIP to study the electrical polarization, since the left-handed SnIP will possess the same FE properties as the right-handed one. Our DFT calculation indicates the lattice constant of $\vec{a}$ as shown in Fig. 1(a) is 8.12 Å which is slightly larger than the experimentally observed value of bunched SnIP by 0.19 Å [36]. Considering the interaction between each rod in the bunch will reduce the length along $\vec{a}$, our calculation result is quite reliable. We analyze the Mulliken population of each atom of SnIP, and find that Sn carries 0.45 positive charges while P and I get 0.22 and 0.23 more electrons respectively. This result clearly shows SnIP is an ionic compound, and it could be a potential candidate of FE materials. However the space group of $P2$ of SnIP shows a 180° rotation symmetry in the direction along the axis perpendicular to the helix, which prohibits the polarization in this pristine system. Further modification of the structure is needed to induce ferroelectricity.

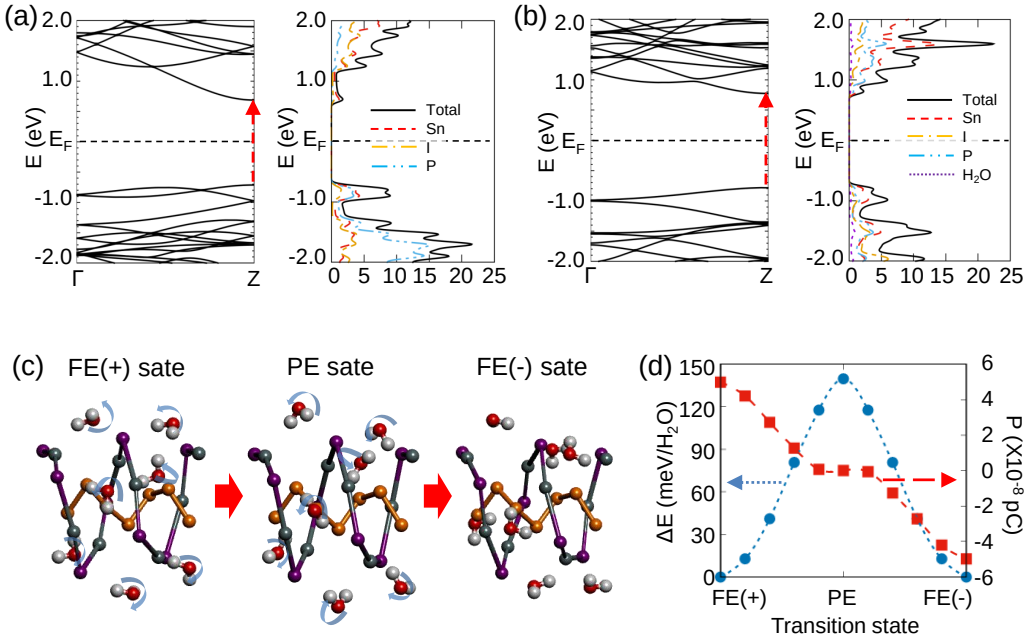


Fig. 3. Electronic band structure (E_k) and density of states (DOS) including its projection on individual atoms (left panels) for (a) optimum 1D double-helix SnIP, (b) $(H_2O)_7$@SnIP. (c) Illustration of flipping ferroelectricity of $(H_2O)_7$@SnIP, FE(+) sate and FE(-) state are energetic eigenvalue states with opposite polarization direction. PE state is the intermediate paraelectric state. (d) The change of energy and polarization in the process of transformation from FE(+) to FE(-) state.

An in-depth analysis of the double-helix SnIP reveals that for the outer helix SnI, there are two types of regions namely $R1$ and $R2$, which are highlighted by blue and red shadows respectively in Fig. 1(b). In one primitive unit cell of SnIP, there are seven alternatively arranged $R1$ and $R2$ regions. For each region, it is surrounded by two Sn atoms and two I atoms. $R1$ is enclosed by I_1-Sn_1-I_2-Sn_2, and $R2$ is enclosed by Sn_2-I_2-Sn_3-I_3. In $R1$, the distance d between two I atoms $d(I_1\text{-}I_2)$=4.92 Å, and d between two Sn atoms $d(Sn_1\text{-}Sn_2)$=5.41 Å, while in $R2$, $d(I_3\text{-}I_2)$=5.81 Å and $d(Sn_3\text{-}Sn_2)$=4.42 Å. These two different regions offer two different potential spaces. Then we investigate the absorption of water molecules on the surface of the outer helix SnI. We first put one water molecule in $R1$ and $R2$ to see which region the water molecule prefers to stay. When water molecules are absorbed in $R1$ or $R2$, the two hydrogen (H) atoms of water molecule are attracted by two I atoms, and the oxygen (O) atom tilts to one of the two Sn atoms. In other words, $R1$ and $R2$ provide a double-well potential for water molecules. As a result, there are two configurations for one water molecule attached in $R1$ or $R2$,

labeled by $R1-1$, $R1-2$, $R2-1$ and $R2-2$ shown in Fig. 1(b). Our DFT-PBE calculations indicate that the cohesive energy of $\Delta E_{PBE}(R1-1) = 275$ meV, $\Delta E_{PBE}(R1-2) = 277$ meV, $\Delta E_{PBE}(R2-1) = 298$ meV and $\Delta E_{PBE}(R2-2) = 299$ meV. Taking the DFT calculation error of energy into consideration, we can conclude that the configuration of $R1-1$ is as energetically stable as $R1-2$ and $R2-1$ is as energetically stable as $R2-2$. Considering SIESTA uses pseudo-atomic-orbital basis sets, the cohesive energy will be overestimated due to the basis set superposition error (BSSE). We have done correction calculations for BSSE (BSSEc), and find that $\Delta E_{PBE-BSSEc}(R2) = 150$ meV and $\Delta E_{PBE-BSSEc}(R1) = 135$ meV. We also use DFT-LDA to calculate the cohesive energy with BSSE correction taken in account, and find that $\Delta E_{LDA-BSSEc}(R2) = 426$ meV and $\Delta E_{LDA-BSSEc}(R1) = 398$ meV. Both the results of DFT-PBE and DFT-LDA show that the configuration of water molecule staying in $R2$ is more stable than in $R1$. From previous works [40,41], we should claim here that the real cohesive energy of $\Delta E(R2)$ should be between 150 meV and 426 meV. The mulliken charge analysis of configurations in $R2$ shows a charge transfer from water molecule to SnIP with 0.03 e.

Then we investigate two molecules absorbed in two neighboring $R2$ regions of SnIP separately. We find that the two water molecules aligning in the same direction are more stable than aligning in the opposite direction by 34 meV. Next, we focus on the water molecules aligning in the same direction while staying on SnIP. As mentioned above, in one primitive unit cell of SnIP, there are seven $R2$ regions available for water molecules to stay. We assume the simplest case that each $R2$ region only absorbs one water molecule. The formed chemical formula is written as $(H_2O)_7$@SnIP as the atomic structure shown in Fig. 2(a). The cohesive energy of absorbing seven water molecules in $R2$ regions in one unit cell is $\Delta E(R2) = 295$ meV. The cohesive energy $\Delta E(R2)$ is stronger than a typical van der Waals interaction, which not only locks the molecule in a specific orientation, but also results in the distortion in atomic structure of SnIP. After absorbing seven water molecules in one unit cell, the system is elongated by 4.4%. The dynamic stability of $(H_2O)_7$@SnIP is confirmed by the phonon spectrum shown in Fig. 2(c).

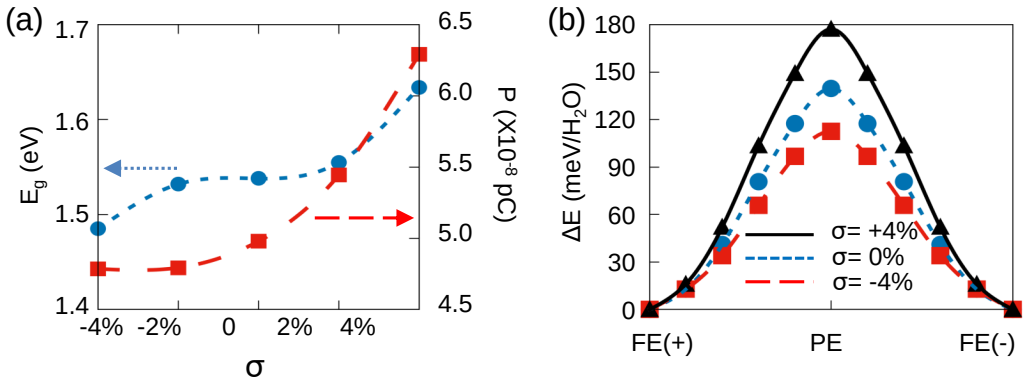


Fig. 4. (a) Band gap value E_g and the polarization as function of the axial strain. (b) The change of energy in the process of transformation from FE(+) to FE(-) state with axial strain of -4%, 0% and $+4\%$.

Band structure and ferroelectric behavior of $(H_2O)_7$@SnIP

The isolated SnIP is a semiconductor with a direct band gap of 1.32 eV at Z-point shown in Fig. 3(a). We should claim here that the bandgap is underestimated by DFT-PBE calculation, but still provides useful insights into the trend in the electronic structures. For $(H_2O)_7$@SnIP, a direct band gap of 1.48 eV at Z-point is shown in Fig. 3(b). The dispersion relation at the top of valence bands and bottom of conduction bands is

similar for both systems, which may come from SnIP but not water molecule. This is confirmed by the partial density of state in Fig. 3(a) and (b), where we can see that the contribution from water is almost zero in the energy range from -2 eV to 2 eV. So while the SnIP is stretched after absorbing water molecules, the orbital hopping of SnIP is reduced, which results in an increase of bandgap by 0.16 eV.

To study the ferroelectricity, we first analyze the detailed shift of each atoms of the system. After combining water molecules and SnIP, besides the oriented arrangement of water molecules and the stretch of SnIP resulted by the interaction, there is also a local displacement of atoms. We compare the atomic structure of SnIP in $(H_2O)_7$@SnIP with the isolated SnIP stretched by 4.4%. We find an obvious displacement of I atoms by 0.3 Å along the axis direction, while the displacement of Sn and P atoms can be ignored. The illustration of the shift of I atoms is represented by the red arrow in Fig. 2(a). Besides the displacement of I atoms along the axis direction, there is also a slight shift of I atoms in the plane perpendicular with the axis. These distortions of atomic structure make the space group $P2$ of pristine SnIP change to space group $P1$ of SnIP in $(H_2O)_7$@SnIP.

The ferroelectricity of the system can be divided into two main parts. The first one is the arrangement of the dipole of water molecules. Since the H_2O is an ionic molecule, the polarization of water molecule $P(H_2O)$ can be defined as the charge of O ion times the distance between the center of positive and negative charge. Since the center of positive and negative charge is overlapped in the pristine SnIP, there is no net polarization. After absorbing the water molecules, we see the displacement of I ion carrying 0.22 negative charges, then $P(SnIP)$ is defined as the charge of I ion times the shift of I ion. P_Z is the decomposition of P in the Z direction. In the DFT calculation, we usually use berry phase method installed in the software to calculate the polarization directly. From Fig. 2(a), we see the component of water dipole along axis $P_Z(H_2O)$ is in the negative Z-direction, and the shift of I atoms in the negative Z-direction results in an electric dipole P_Z(SnIP) in the positive Z-direction. If we do not consider the charge redistribution between atoms caused by absorbing water molecule on SnIP, the total net electric polarization P_Z should be the difference between P_Z(SnIP) and $P_Z(H_2O)$. We first separate the 1D water wire and the SnIP, and then calculate P_Z. We find that $P_Z(H_2O)=3.61\times10^{-8}$ pC and P_Z(SnIP)$=6.53\times10^{-8}$ pC respectively, so $P_Z = 2.92\times10^{-8}$ pC. However, the charge redistribution can not be neglected, and it will modify $P_Z(H_2O)$ and P_Z(SnIP). We study the charge Q of atoms before and after absorbing water molecules on SnIP. Q(O) decrease from -0.78 to -0.73, Q(H) of half of H atoms decrease from 0.39 to 0.36, while the charge of other half keeps the same, the decrease of charges of H and O results in the decrease of electric dipole of the water molecule. Instead, Q(Sn) increases from 0.45 to 0.47 and Q(I) increases from -0.23 to -0.27, which makes an increase of dipole moment of SnIP. As a result, the increase of P_Z(SnIP) and the decrease of $P_Z(H_2O)$ lead to a larger P_Z than 2.92×10^{-8} pC. In order to get a reliable result, we use the standard Berry phase method and get $P_Z = 4.98\times10^{-8}$ pC, which confirms the effect of charge redistribution on the polarization. This electrical polarization of $(H_2O)_7$@SnIP is comparable with the value in $BaTiO_3$ of 3.2×10^{-8} pC [37]. Besides the shift along the axial direction, I atoms also shift in the plane perpendicular to the axis, however these shift are so small that the resulted polarization is negligible.

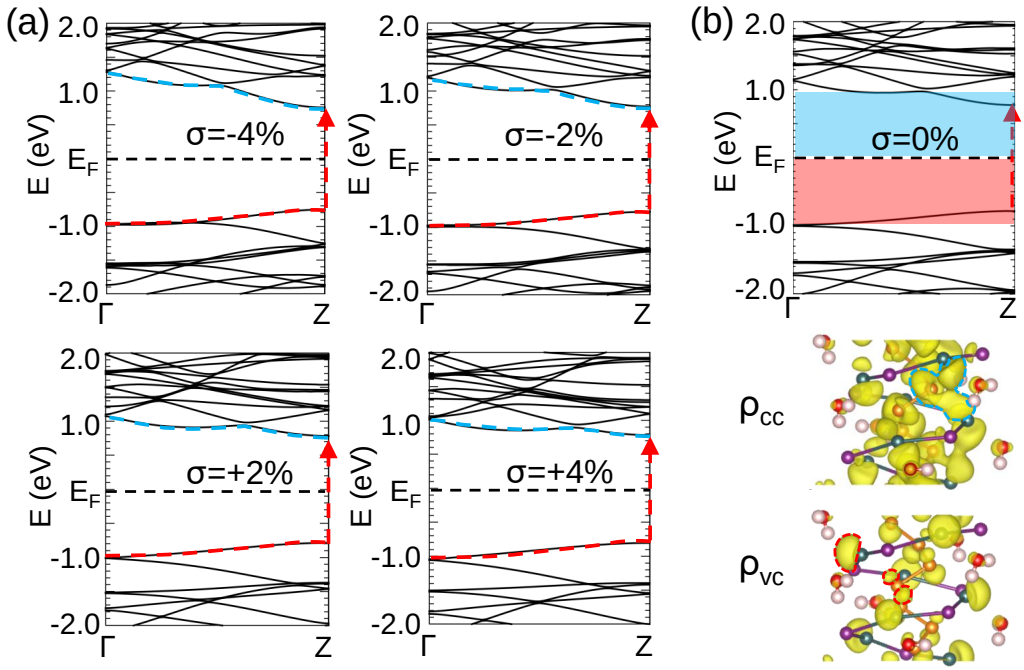


Fig. 5. (a) Band structure E_k of $(H_2O)_7$@SnIP under axial strain. The top valence band is marked by red dashed line and the bottom conduction band is marked by blue dashed line. (b) Charge density associated with valence state ρ_{vc} and conduction state ρ_{cc} of optimum $(H_2O)_7$@SnIP is present in the up and bottom panel respectively. The energy range associated with ρ_{vc} is indicated by the red transparent region in the band structure of optimum $(H_2O)_7$@SnIP extends from $E_F - 0.94 < E < E_F$, and the energy range associated with ρ_{cc} is indicated by the blue transparent region in the band structure of optimum $(H_2O)_7$@SnIP extends from $E_F < E < E_F + 0.94$. The isosurface values of ρ_{vc} and ρ_{cc} are $1{\times}10^{-3}$e/Å^3 and $0.5{\times}10^{-3}$e/Å^3.

While applying an external electric field in the opposite direction with the polarization of a FE material, the polarization can be turned over by 180°. In the process of flipping the polarization, the system starts from the initial FE state FE(+), goes through a PE phase in which there is no net polarization, and arrives at the final FE state FE(-). FE(-) has an opposite polarization but the same energetic stability as FE(+). In the traditional 3D or 2D FE materials like $BaTiO_3$, the PE phase is typically around the midpoint of a linear combination of the FE(+) and FE(-). However, in the PE phase acquired through this way in our system, the bond angle of H-O-H in the water molecule is around 180°, far from the optimum bond angle. As expected, the energy of PE phase is much higher than FE phase by 4.65 eV/H_2O, which means the PE phase obtained through linear combination is not acceptable.

We propose here another reasonable scenario of flipping the electrical polarization as shown in Fig. 3(c). In this scenario, the water molecule is rolling-over while keeping the dipole constant, but changing the direction. In the PE phase, the dipole of water molecule lies in the radial direction of the double helix. In other words, there is no decomposition of dipole of water in the axis direction. In the process of rolling-over of water molecules, due to the interaction between water molecule and SnIP, the atomic structure of SnIP is also changing. In the PE phase, the shift of I atoms and also the associated polarization disappears. As a result of vanishing of the polarization of water molecule and SnIP, there is no net polarization of the whole system in the axis direction. As mentioned above, we know the adjacent water molecules staying in R2 regions prefer to align in the same direction. In the process of transformation from FE(+) to FE(-), once one water molecule starts to turn over, the other neighboring water molecules will follow to turn over. In other words, the seven water molecules flip collectively in the transformation process. The changes of energy and net polarization along the axis in the

process of flipping the polarization are shown in Fig. 3(d). The energy barrier is about 140 meV/H_2O which is about thirty-three times smaller than that of the linear combination scenario.

Strain effect on Ferroelectricity and band structure

We also study the response of ferroelectricity and band structure to the axial strain to explore the perspective of the materials in application. The response of P_Z to the tensile strain is more obvious than the compressive strain. From red dashed line in Fig. 4(a), we see P_Z increases significantly by 26.3% with 4% stretch strain, but decreases very slightly by 4.4% with 4% compress strain. The band gap E_g of the system is also decreased to 1.49 eV with the 4% axial compression and increased to 1.63 eV with 4% axial stretching. The effect of strain on the band gap is shown with blue dotted line in Fig. 3(c). The deformation energy ΔE with strain of 4% is about 70 meV, which means this double-helix can be deformed easily by applying an axial stress. The energy barrier ΔE in the process of transformation from FE(+) to FE(-) is also affected by the strain. As shown in Fig. 4(b), from 4% compressive strain to 4% tensile strain, ΔE is increased from 112 meV/H_2O to 177 meV/H_2O.

The change of the band gap with applying strain may come from the change of band width. In order to explore the physics behind, we calculate the band structures of $(H_2O)_7$@SnIP with different stress conditions as shown in Fig. 5(a). Comparing with the band structure of the system without strain, we find the top valence band highlighted by the red dashed line almost remains unchanged. The width of bottom conduction band highlighted by blue dashed line changes but still keeps the dispersion relation. In Fig. 5(b), the energy range between E_F and 0.2 eV below the top of valence band indicated by the red region, and the 0.2 eV above the bottom of conduction band indicated by the blue region, are used to identify the valence and conduction frontier states. We characterize the charge density associated with valence frontier state ρ_{vc} and conduction frontier state ρ_{cc} in the lower panel of Fig. 5(b). The valence frontier states encircled by red dashed line is mainly occupied by the lone pair orbital of Sn and p_z orbital of P. The conduction frontier states encircled by blue dashed line contain the overlap of orbital of one P atom and two nearest-neighboring Sn atoms. While applying strain on the system, the distances between atoms are changed. Since the valence frontier state has little relation with overlap of orbital of atoms, there should be little change of the top valence band. However, the change of distance affects the overlap of orbital between P and Sn atoms, so we see the change of conduction band. While stretching the system, the distance between two nearest-neighbor Sn atoms is enlarged from 4.54 Å to 4.61 Å, and the distance between P atom and its nearest-neighbor Sn atom is enlarged from 3.46 Å to 3.56 Å. As a result, the overlap between orbital and the resulted width of conduction band is decreased, and vice versa for the compressive strain.

Discussion

When we study the ferroelectric behavior, band structures and their response of axial strain in 1D $(H_2O)_7$@SnIP, one basic question may arise. Is SnIP hydrophilic or hydrophobic and could SnIP attract water molecule from a water cluster? The answer is determined by the competition between the absorption energy of water molecule on SnIP and the interaction between water molecules in water cluster. There are many configurations of water clusters, such as the well known water dimmer. Using PBE-BSSEc, we calculate the interaction between water

molecules $E_{PBE-BSSEc}$ in the dimmer configurations. It ranges from 46 meV to 246 meV. In our system, the interaction energy between water and SnIP is about 150 meV, which holds a great promise for water molecule to stay.

Usually, for a semiconductor, while using strain to improve one physical property, other properties will be degraded. In this study, we find that the modification of polarization by axial strain is very prominent, while the effect of strain on band structure including the dispersion relation and band gap is negligible. So with strain, the polarization is changed while other physical properties are intact. Besides the strain along axis direction, the other common strain occurs frequently in 1D system is bending. In theoretical models of DFT calculation, it will contain too many atoms to study the bending effect on physical properties. However, we can analysis the bending effect qualitatively through the studying effect of axial tensile/compressive strain. The diameter of 1D $(H_2O)_7$@SnIP is about 8.2 Å, which is the same as (6,6) carbon nanotube. When applying the bending strain, the outer part of this 1D double-helix is stretched and the inner part is compressed. If we consider the bending 1D tube as a part of a circle, then the extent of stretch of the outer part is the same with the extent of compression of the inner part. From Fig. 3(c), the response of polarization to tensile strain is much more significant than the response to compressive strain. As a result, we can conclude that the polarization will also be increased by bending the 1D $(H_2O)_7$@SnIP.

The special atomic structure of SnIP makes it to be a promising candidate to explore ferroelectricity in 1D. Here we use water molecule to introduce electrical polarization in SnIP. The double potential well in $R2$ of SnIP enforces the water molecule to arrange in a special orientation. We can use other polarized molecules to replace water molecules, and it will have similar results. In addition, we can use transition metal atoms to dope SnIP. With appropriate choice of transition metal element, the atoms will stay in one of the double-potential wells of SnIP to generate the ferroelectricity. Besides, the doping of transition metal element will also bring magnetism to the 1D system.

4. Conclusion

In conclusion, we have identified ferroelectricity induced in 1D direct-gap semiconductor $(H_2O)_7$@SnIP through absorbing water molecule in SnIP. Our *ab initio* DFT calculations indicate that there are two double-potential well regions $R1$ and $R2$ of SnIP for water molecule to stay, and water molecule prefer to attach in $R2$. The water molecules are arranged in a special orientation due to the double-potential well of $R2$. On the other hand, the interaction between water molecule and SnIP will lead to the distortion of the atomic structure of SnIP and also a charge redistribution between atoms. Comparing with the pristine SnIP with space group of $P2$, $(H_2O)_7$@SnIP with space group of $P1$ loses the 180° rotation symmetry. For polarization flipping mechanism, we propose a scenario in which the water molecules rotate while keeping the magnitude of the dipole but changing the direction. The rotation of water molecule also leads to the deformation of atomic structure of SnIP. When the dipole of water molecule lies in the radial direction, SnIP is transformed back to the phase with space group of P2. As a result, the net polarization along the axis direction disappears. The effect of external axial strain on polarization is quite remarkable, with 4% stretching, the polarization is enhanced by about 26%. However the response of E_g of the band structure to the axial strain is not significant, since only the bottom of conduction band, instead of top of the valence band, correlates with orbital overlap of atoms.

Acknowledgment

D. Liu, R. Wei and L. Han acknowledges financial support by the Natural Science Foundation of the Jiangsu Province Grant No. BK20210198. S. Dong acknowledge financial support by the National Natural Science Foundation of China (NNSFC) Grant No. 11834002. Computational resources for most calculations have been provided by the Michigan State University High Performance Computing Center.

References

[1] Rabe K M, Ahn C and Triscone J M 2007 *Physics of ferroelectrics : a modern perspective* (Berlin: Springer)

[2] Choi K J, Biegalski M, Li Y L, Sharan A, Schubert J, Uecker R, Reiche P, Chen Y B, Pan, X Q, Gopalan V, Chen L-Q, Schlom D G, Eom C B 2004 Science **306** 1005

[3] Fei R, Kang W and Yang, L. 2016 Phys. Rev. Lett. **117** 097601

[4] Tian Z, Guo C, Zhao M, Li R and Xue J 2017 ACS Nano **11** 2219

[5] Wang H and Qian X 2017 2D Mater. **4** 015042

[6] Guan Z, Hu H, Shen X, Xiang P, Zhong N, Chu J and Duan C 2020 Adv. Elec. Mater. **6** 1900818

[7] Ding W, Zhu J, Wang Z, Gao Y, Xiao D, Gu Y, Zhang Z and Zhu W 2017 Nat. Comm. **8** 14956

[8] Liu F, You L, Seyler K L, Li X, Yu P, Lin J, Wang X, Zhou J, Wang H, He H, Pantelides S T, Zhou W, Sharma P, Xu X, Ajayan P M, Wang J and Liu Z 2016 Nat. Comm. **7** 12357

[9] Xiao J, Zhu H, Wang Y, Feng W, Hu Y, Dasgupta A, Han Y, Wang Y, Muller D A, Martin L W, Hu P A and Zhang X 2018 Phys. Rev. Lett. **120** 227601

[10] Li L and Wu M 2017 ACS Nano **11** 6382

[11] Ding N, Chen J, Gui C, You H, Yao X and Dong S 2021 Phys. Rev. Materials **5** 084405

[12] Song S, Zhang Y, Guan J and Dong S 2021 Phys. Rev. B **103** L140104

[13] Wang Z, Ding N, Gui C, Wang S, An M and Dong S 2021 Phys. Rev. Materials **5** 074408

[14] Ding N, Chen J, Dong S and Stroppa A 2020 Phys. Rev. B **102** 165129

[15] Lin L, Zhang Y, Moreo A, Dagotto E and Dong S 2019 Phys. Rev. Lett. **123** 067601

[16] You Lu, Zhang Y, Zhou S, Chaturvedi A, Morris S A, Liu F, Chang L, Ichinose D, Funakubo H, Hu W, Wu T, Liu Z, Dong S and Wang J 2019 Sci. Adv. **5** eaav3780

[17] Wu M, Burton J D, Tsymbal E Y, Zeng X C and Jena P 2013 Phys. Rev. B **87** 081406(R)

[18] Kan E, Wu F, Deng K and Tang W 2013 Appl. Phys. Lett. **103** 193103

[19] Lin L, Zhang Y, Moreo A, Dagotto E and Dong S 2019 Phys. Rev. Materials **3** 111401(R)

[20] Hernandez Y, Pang S, Feng X and Mullen K 2012 Elsevier 415

[21] Iijima S and Ichihashi T 1993 Nature **363** 603

[22] Iijima S 1991 Nature **354** 56

[23] Ren Y and Wu M 2021 J. Chem. Phys. **154** 044705

[24] Zhang J, Guan J, Dong S and Yakobson B I 2019 J. Am. Chem. Soc. **141** 15040

[25] Zhang L, Tang C, Sanvito S and Du A 2021 Npj Comput. Mater. **7** 135

[26] Zhao H, Kong X, Li H, Jin Y, Long L, Zeng X, Huang R and Zheng L 2011 Proc. Natl. Acad. Sci. U.S.A. **108** 3481

[27] Pfister D, Schafer K, Ott C, Gerke B, Pottgen R, Janka O, Baumgartner M, Efimova A, Hohmann A, Schmidt P, Venkatachalam S, van Wullen L, Schurmann U, Kienle L, Duppel V, Parzinger E, Miller B, Becker J, Holleitner A, Weihrich R and Nilges T 2016 Adv. Mater. **28** 9783

[28] Hoff D A and Rego L G C 2021 Nano Lett. **21** 8190

[29] Artacho E, Anglada E, Dieguez O, Gale J D, Garcia A, Junquera J, Martin R M, Ordejon P, Pruneda J M, Sanchez-Portal D and Soler J M 2008 J. Phys.: Condens. Matter **20** 064208

[30] Perdew J P, Burke K and Ernzerhof M 1996 Phys. Rev. Lett. **77** 3865

[31] Troullier N and Martins J L 1991 Phys. Rev. B **43** 1993

[32] Monkhorst H J and Pack J D 1976 Phys. Rev. B **13** 5188

[33] Hestenes M R and Stiefel E 1952 J. Res. Natl. Bur. Stand. **49** 409

[34] Resta R, Posternak M and Baldereschi A 1993 Phys. Rev. Lett. **70** 1010

[35] Resta R and Vanderbilt D 2007 Springer Berlin Heidelberg 31

[36] Pfister D, Schafer K, Ott C, Gerke B, Pottgen R, Janka O, Baumgartner M, Efimova A, Hohmann A, Schmidt P, Venkatachalam S, van Wullen L, Schurmann U, Kienle L, Duppel V, Parzinger E, Miller B, Becker J, Holleitner A, Weihrich R and Nilges T 2016 Adv. Mater. **28** 9783

[37] Ren X 2004 Nat. Mater. **3** 91

[38] Santra B, Michaelides A and Scheffler M 2007 J. Chem. Phys. **127** 184104

[39] Gillan M J, Alfe D and Michaelides A 2016 J. Chem. Phys. **144** 130901

[40] Lee K, Yu J and Morikawa Y 2007 Phys. Rev. B **75** 045402

[41] Liu D, Guan J, Jiang J, and Tomanek D 2016 Nano Lett. **16** 7865

[42] Ceperley D M and Alder B J 2016 Phys. Rev. Lett. **45** 566